Variability of the Great Plains Low-Level Jet: Large-Scale Circulation Context and Hydroclimate Impacts

SCOTT J. WEAVER

Department of Atmospheric and Oceanic Science, University of Maryland, College Park, College Park, Maryland

SUMANT NIGAM

Department of Atmospheric and Oceanic Science, and Earth System Science Interdisciplinary Center, University of Maryland, College Park, College Park, Maryland

(Manuscript received 12 July 2006, in final form 29 August 2007)

ABSTRACT

Variability of the Great Plains low-level jet (GPLLJ) is analyzed from the perspective of larger-scale, lower-frequency influences and regional hydroclimate impacts as opposed to the usual analysis of its frequency, diurnal variability, and mesoscale structure. The circulation-centric core analysis is conducted with monthly data from the high spatiotemporal resolution, precipitation-assimilating North American Regional Reanalysis, and the 40-yr ECMWF Re-Analysis (ERA-40) (as necessary) to identify the recurrent patterns of GPLLJ variability and their large-scale circulation links. The links are first investigated from regressions of an index representing meridional wind speed in the climatological jet-core region; the core region itself is defined from analysis of seasonal and diurnal variability of the jet structure and moisture fluxes.

The analysis reveals that GPLLJ variability is, indeed, linked to coherent, large-scale, upper-level height patterns over the Pacific and North Atlantic Oscillation (NAO) variability in the Atlantic. A Rossby wave source analysis shows the Pacific height pattern to be potentially linked to tropical diabatic heating anomalies in the west-central basin and in the eastern Pacific sector. EOF analysis of GPLLJ variability shows it to be composed of three modes that, together, account for ~75% of the variance. The modes represent the strengthening/expansion of the jet core (38%), with a strong precipitation impact on the northern Great Plains, and linked to post-peak-phase ENSO variability; meridional shift of the GPLLJ (23%), with a Gulf states precipitation focus, and linked to pre-peak-phase ENSO variability; and in-place strengthening of the GPLLJ (12%), with dipolar influence on Great Plains and Gulf states precipitation, and linked to summer NAO variability.

1. Introduction

The Great Plains of North America extend from the interior Canadian provinces of Alberta, Saskatchewan, and Manitoba southward through the west-central United States into Texas. This area is a predominantly flat agricultural region in close proximity to the Rocky Mountains and the Gulf of Mexico. During spring and summer, large amounts of heat and moisture are transported northward from the Gulf of Mexico into the central United States by the Great Plains low-level jet (GPLLJ). These fluxes and their convergence exert profound influence on the hydroclimate of the Great Plains by providing both moisture and the necessary thermodynamic environment for precipitation formation.

The characterization of regional expressions of global climate variability/change is a high priority of the U.S. Climate Change Science Program, as evidenced by its Water Cycle initiative (Hornberger et al. 2001). Improved understanding of Great Plains hydroclimate variability leading to enhanced prediction skill is a key initiative goal. The GPLLJ figures prominently in this initiative, given the dominance of moisture transports over local evaporation in generation of summer precipitation variability over the Great Plains (Ruiz-Barradas and Nigam 2005, hereafter RBN05).

Corresponding author address: Scott J. Weaver, 4337 Computer and Space Sciences Bldg., University of Maryland, College Park, College Park, MD 20742-2425.
E-mail: sweaver@atmos.umd.edu

DOI: 10.1175/2007JCLI1586.1

The GPLLJ is a persistent, warm-season climatic feature characterized by a wind maximum below 850 hPa. The jet typically develops at night, but its robust amplitude and prevalence in spring/summer months enables the jet signature to be manifest in the monthly averaged wind field (Higgins et al. 1997; Mo et al. 1997; Stensrud 1996). The GPLLJ develops due to supergeostrophic wind speeds, as a consequence of spatially uneven and diurnally varying heating of terrain slopes, boundary layer frictional effects, and inertial oscillation of the ageostrophic wind vector (Blackadar 1957; Holton 1967; Hoxit 1975; Wexler 1961). Uccellini and Johnson (1979) showed that the GPLLJ was influenced also by the upper-level synoptic flow; in particular, jet streaks and related secondary circulations.

Although diurnal boundary layer influences are important for jet formation, the larger-scale, slowly varying circulation (e.g., monthly flow) on which diurnal influences superpose can be important for jet variability. Byerle and Paegle (2003) show North American orography to be influential in focusing global-scale flow features into regional responses, especially GPLLJ modulations. Stationary wave modeling also shows mechanical blocking of the Atlantic trade winds and related potential vorticity conservation to be the primary mechanism for GPLLJ development, with diurnally varying thermal influences being secondary (Pan et al. 2004; Ting and Wang 2006). In view of these findings, it is important to consider the low-frequency (i.e., supersynoptic) variations of the GPLLJ: their structure, origin, and hydroclimate impacts.

Seasonal and subseasonal strength of the GPLLJ has indeed been shown linked with Great Plains hydroclimate via moisture fluxes (Helfand and Schubert 1995; Higgins et al. 1997; Schubert et al. 1998). Anomalous warm-season precipitation over the United States has been associated with large-scale circulation variability originating in the Pacific, along with contemporaneous variations of the GPLLJ (Mo et al. 1995; Bell and Janowiak 1995; Trenberth and Guillemot 1996; Mo et al. 1997). The Atlantic also influences summer rainfall over the Great Plains, again via low-frequency modulation of the GPLLJ (RBN05).

The GPLLJ's influence on moisture transports and low-level moisture flux convergence, along with emerging evidence from observational and modeling studies for remote influences on Great Plains precipitation, calls for the characterization of recurrent structures of GPLLJ variability and their dynamic and thermodynamic links to remote regions. Issues examined here include the following:

- Is GPLLJ variability linked to larger-scale, lower-frequency summer circulation variability, for example, over the North Pacific–North American region?
- What is the structure of regional precipitation anomalies associated with GPLLJ variability?
- What are the recurrent patterns of GPLLJ variability? Does the jet core expand meridionally or zonally? Which of these patterns is of consequence for Great Plains rainfall?

This study is complementary to RBN05 in that a circulation-centric analysis strategy is adopted here. This strategy is, in fact, suggested by the precipitation-centric analysis of RBN05, which showed remote water sources to be important in Great Plains hydroclimate variability. As water from remote regions (e.g., Gulf of Mexico) is transported into the continental interior, most effectively by the GPLLJ, this circulation feature and its variability is the analysis focus, with the ultimate objective of understanding the origin of warm-season hydroclimate variability over the Great Plains.

The dataset of choice for studying the GPLLJ structure and variability is the recently released North American Regional Reanalysis (NARR; Mesinger et al. 2006). In contrast with global reanalyses, NARR has finer spatiotemporal resolution and an improved data assimilation strategy, including direct assimilation of precipitation and radiances. The precipitation assimilation is, in fact, quite successful, raising the prospects of improved land surface state representation in this dataset. These enhancements should lead to more accurate depictions of the GPLLJ structure and variability, given the considerable influence of surface fluxes on low-level-jet development in mesoscale modeling experiments (Zhong et al. 1996; Zhang et al. 2006). NARR is thus the preferred dataset for the GPLLJ-related hydroclimate analysis. The large-scale circulation context for GPLLJ variability is, of necessity, analyzed using the global 40-yr European Centre for Medium-Range Weather Forecasts (ECMWF) Re-Analysis (ERA-40).

The present study focuses on the larger-scale, lower-frequency influence on GPLLJ variability; as opposed to canonical analysis of jet frequency and mesoscale structure. The "supersynoptic" analysis framework is a defining attribute of the study. Surely, the monthly statistics will not capture mesoscale aspects of jet variability, but that is by design. Interesting as it is, mesoscale evolution and dynamics of the GPLLJ is not the focus of this study, whose salient features are as follows:

- investigation of seasonal and interannual GPLLJ variability using the high spatiotemporal resolution and precipitation-circulation consistent 24-yr NARR data record;
- creation of a GPLLJ index to study interannual variability;
- characterization of the GPLLJ links to local and larger-scale circulation features, diabatic heating, and Great Plains hydroclimate;
- identification of recurrent modes of GPLLJ variability from EOF analysis and characterization of their circulation and hydroclimate links.

Focusing on monthly anomalies over the Great Plains may seem problematic given the dramatic onset of the North American monsoon in June/July with attendant effects over the Great Plains region (e.g., Barlow et al. 1998). However, our analysis demonstrates that monthly anomaly statistics shows no calendar month preference during the warm season over the Great Plains. For example, precipitation variability is also uniformly distributed in these months: the Great Plains precipitation index standard deviations are 1.1, 1.09, and 1.08 mm day^{-1}, respectively (e.g., RBN05).

The data sources and analysis methods are described in section 2. The low-level flow structure and moisture-flux characteristics associated with the climatological GPLLJ are discussed in section 3. Section 4 presents the GPLLJ index while its regressions on dynamical and thermodynamical fields, including regional precipitation, are shown and discussed in section 5. Recurrent variability of the GPLLJ and related hydroclimate footprints are presented in section 6, while a brief summary of findings and suggestions for future work follow in section 7.

2. Datasets and methodology

a. Datasets

The North American Regional Reanalysis is a 25-yr (1979–2003), consistent, high-resolution dataset that covers the North American domain (Mesinger et al. 2006). A striking difference between the NARR and National Centers for Environmental Prediction (NCEP) reanalysis is spatiotemporal resolution; NARR has a 3-h analysis cycle and 32-km horizontal resolution. There are 13 vertical levels below 700 hPa in NARR, which helps resolve the GPLLJ features. Additionally, and more importantly, NARR assimilates direct observations of precipitation over land by nudging the precipitation, moisture, temperature (diabatic heating), and cloud water mixing ratio variables.

The ERA-40 global reanalysis covers a 44-yr period beginning September 1957. It was produced at the ECMWF (Uppala et al. 2005) from conventional observations and satellite data streams. Analyses were produced at 6-hourly intervals and archived on a 2.5° horizontal grid and 23 isobaric levels, ranging from 1000 to 1 hPa, with 12 levels below 150 hPa.

Diabatic heating has been diagnosed in-house from three global reanalyses (NCEP, ERA-15, and ERA-40; Nigam et al. 2000; Chan and Nigam 2008, manuscript submitted to *J. Climate*) as a residual in the thermodynamic equation (e.g., Hoskins et al. 1989; Nigam 1994), using monthly averaged data and submonthly transient fluxes. Heating was diagnosed with/without mass balancing, with minimal differences. The ERA-40 diagnosis was performed at the resolution of the isobaric archives (2.5° resolution).[1]

b. Methodology

Climatological analysis is conducted using monthly averaged meridional wind and the column meridional moisture flux; the column integral is defined as the mass-weighted integral from 1000 to 700 hPa. A GPLLJ variability index is developed from the jet-core region departures of the 900-hPa meridional wind from its monthly climatology. Links with precipitation are ascertained using the Great Plains precipitation index (cf. RBN05), defined as the average precipitation in the region north of the jet core (35°–45°N, 90°–100°W). Monthly regressions are computed on selected fields, including vertically averaged diabatic heating (from ERA-40 residual diagnosis) and SST [from the Hadley Centre Global Sea Ice and SST (HadISST) dataset; Rayner et al. 2006].

The recurrent patterns of GPLLJ variability are identified from EOF analysis, performed on 900-hPa monthly meridional winds over the Great Plains. A covariance-based analysis on $(\cos\theta)^{1/2}$ weighted field (θ is latitude, to ensure grid-area parity) was performed. The EOFs are not rotated given the limited analysis domain. The principal components obtained from this analysis are used in relating GPLLJ variability to regional hydroclimate and larger-scale circulation variability via regressions. The EOF analysis can reveal the modal mix manifest in GPLLJ index variations, and thus advance dynamical understanding of jet variability.

[1] Interpolating fields from native spectral representation to latitude–longitude grid must surely introduce additional uncertainty in heating estimates, but this cannot be large given the close correspondence of diagnosed and archived heating fields in NCEP reanalysis, at least over the central tropical Pacific (cf. Fig. 10 in Nigam et al. 2000).

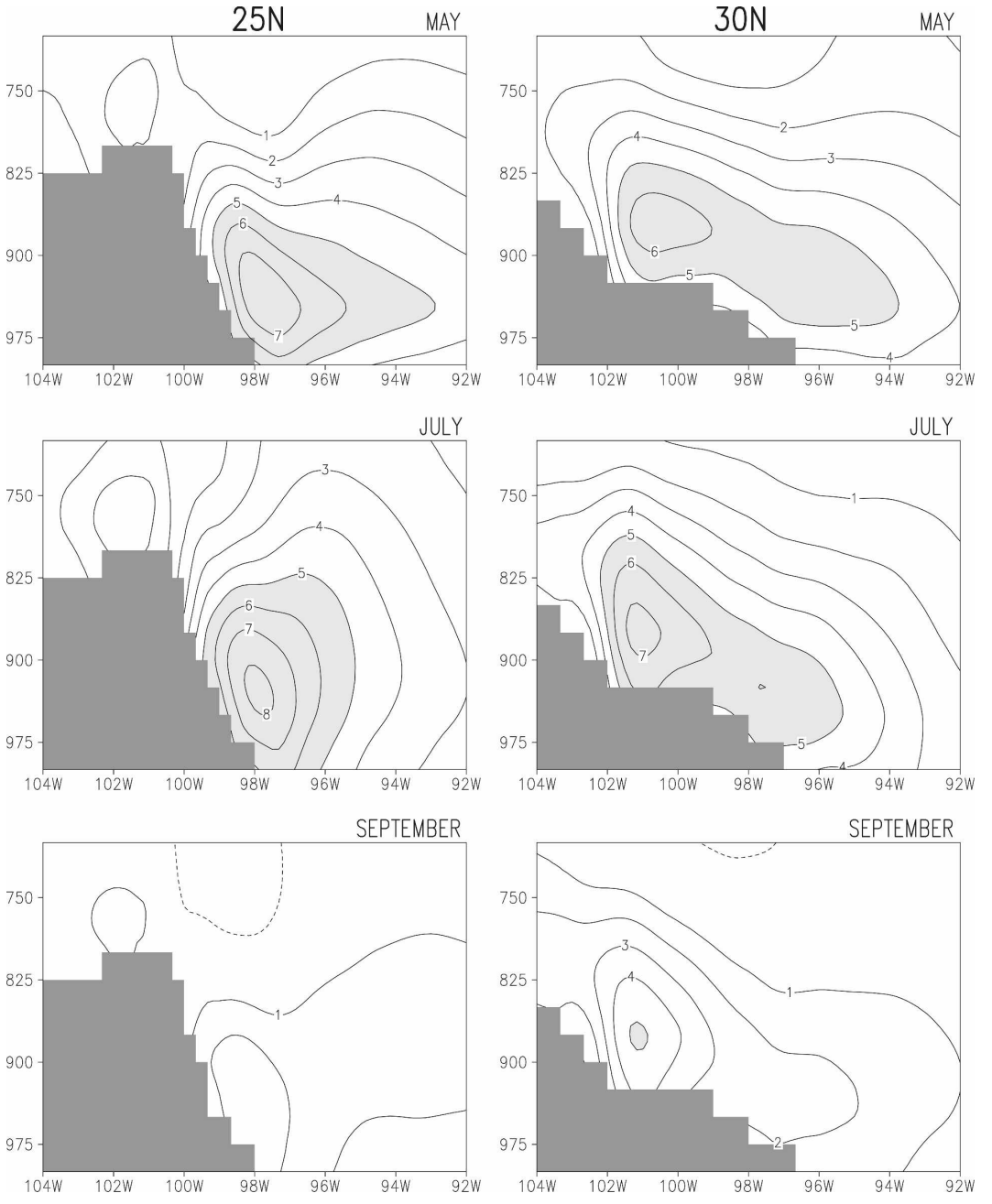

FIG. 1. Seasonal evolution of the Great Plains low-level jet. Meridional wind at (left) 25° and (right) 30°N in NARR at approximately 0.3° × 0.3° horizontal and 25-hPa vertical resolution. Contours >5 m s^{-1} are shaded. Topography is blocked out.

3. Great Plains low-level jet: Seasonal variability

a. Jet profile

Longitude–height cross sections of monthly meridional wind at 25° and 30°N are shown in Fig. 1, for May, July, and September. Significant vertical wind shear is present above the jet core at both 25° and 30°N, except in September. The jet maximum increases with the advance of the warm season, peaking in July at both latitudes. The jet core is located between 900 and 950 hPa at 25°N but somewhat higher (900–850 hPa) at 30°N. The core is tightly packed at 25°N, likely because of steep topography to the west. Topography is known to impact the jet structure from generation of shallow baroclinicity on its slopes (e.g., Zhang et al. 2006). At 30°N, the core has shifted to the west and exhibits a

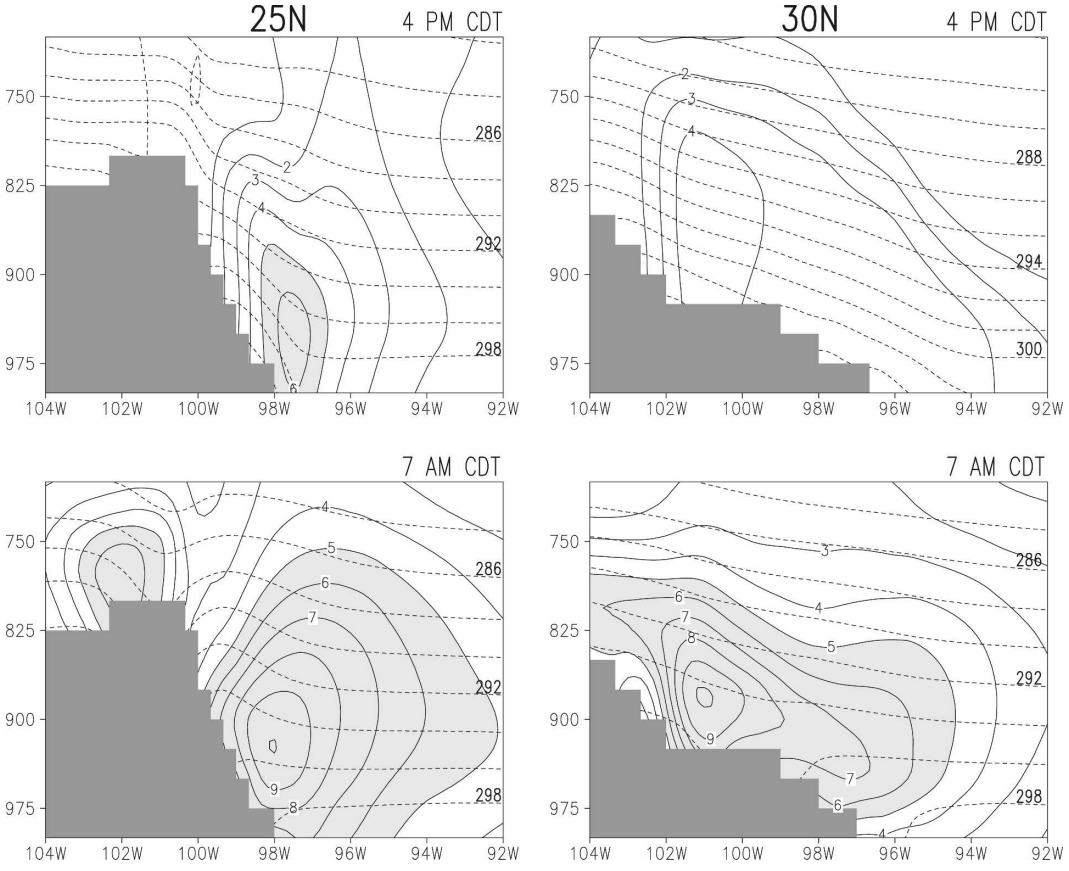

FIG. 2. Diurnal variability of the Great Plains low-level jet in July. Meridional wind (solid) and temperature (K) (dashed) at (left) 25° and (right) 30°N for 4 p.m. and 7 a.m. LT in NARR. Contour intervals are 1 m s^{-1} and 2 K. Contours >5 m s^{-1} are shaded. Horizontal and vertical resolution is the same as in Fig. 1.

more gradual eastward downward slope, reflecting the underlying terrain slope and related thermal attributes. The seasonal demise of the LLJ in August–September is gradual at 30°N, but notably precipitous at 25°N.

b. Diurnal cycle

Figure 2 displays longitude–height cross sections of the July meridional wind (contoured) and temperature (dashed) fields at the time of minimum [4 p.m. central daylight time (CDT)] and maximum (7 a.m. CDT) jet magnitude.[2] The late afternoon to early morning development in jet speed and extent is striking. Previous studies have noted a nighttime doubling of wind speed (e.g., Stensrud 1996), and while NARR does not generate quite a doubling in the monthly averaged diurnal cycle at 25°N (from 6 to 9 m s^{-1}), it does so at 30°N (from 4 to 9 m s^{-1}). The average over all eight 3-hourly NARR time steps in July was shown earlier (middle panels in Fig. 1) and is evidently closer to the 7 a.m. monthly mean, especially at 25°N. This suggests that the monthly mean jet remains strong across many of the eight time steps, and that diurnal variability of the jet increases with latitude.

The thermal structure shows significant diurnal variations, much as anticipated: isotherms slope steeply toward the plains in the afternoon but not in the early morning when a warm dome of air is present along the eastern slopes above the 950-hPa level. Although tempting, one must refrain from verifying the thermal-wind balance between $\partial V/\partial z$ and $\partial T/\partial x$ in Fig. 2. The extent to which geostrophic balance, and thus thermal-wind balance, hold at subsynoptic scales of the GPLLJ and in the planetary boundary layer (PBL) region is unclear; and under investigation. Should the thermal-wind balance be applicable, the eastward down-sloping isotherms in Fig. 2 would imply a northerly thermal

[2] A monthly rendition of diurnal variability is generated by averaging each diurnally stamped data across all the month days, for example, from a 31-day average of 7 a.m. LT July data, and so on.

wind, and thus a diminished GPLLJ at upper levels, more diminished in case of steeper isotherms, in accord with depicted diurnal variations, especially at 25°N. Note that the isotherms are not only less steep during early morning, but their east–west gradient changes sign below 950 hPa in the vicinity of topography. The location of the jet core near this level is again not inconsistent with thermal-wind balance considerations.

c. Meridional water vapor flux

The primary impact of the GPLLJ on hydroclimate is through northward column moisture transport from the Gulf of Mexico, and its subsequent convergence in the jet-exit region. A benefit to viewing the climatological jet in terms of column fluxes is twofold: the variable vertical range of the jet core is accounted for by the vertical integral, and the jet's influence on hydroclimate of the Great Plains is readily apparent.

Figure 3 displays the column-integrated NARR meridional moisture flux in spring and summer months. Enhanced fluxes are present in several regions: modest inflow from the Gulf of Mexico begins in spring and increases through early summer, reaching a peak of 200 kg m^{-1} s^{-1} over northeastern Mexico in July, when its reach into the southern and central Great Plains is greatest. Moisture fluxes associated with monsoonal flow over southwestern United States in late summer, especially the Gulf of California low-level jet,[3] are captured nicely, as are the northward fluxes associated with the westward flank of the Bermuda high, which skirts the eastern seaboard in boreal summer months.

This meridional moisture flux view of the GPLLJ is consistent with its meridional-wind-based depiction (cf. Fig. 1), in that the jet core is located at ~25°N with a northwestward tilt in both descriptions. If meridional fluxes over northeastern Mexico and the south-central United States are primarily due to the GPLLJ, then these fluxes must exhibit diurnal variability akin to the jet. Figure 4 shows the diurnal cycle of the monthly and vertically integrated meridional moisture flux in NARR for May, July, and September as diagnosed from harmonic analysis. The arrow length indicates flux magnitude while the direction denotes the time of day when the flux is a maximum. For example, an arrow pointing due north indicates a flux maximum at 6 a.m. CDT.

The diurnal amplitude of the northward moisture flux is evidently strongest in July over both land and water. Over the Gulf of Mexico (and California) and over the southern tier states, the northward flux is strongest at midnight, but fluxes over central United States and the eastern seaboard are maximum in the wee hours of the morning (~6 a.m. CDT). The reason for clockwise veering of the arrows with increasing latitude over the southern Great Plains is noted with interest. The diurnal cycle of meridional moisture flux has its origin in the diurnal variability of low-level meridional winds; diurnal variability of specific humidity was ascertained to be negligible.

4. Low-level-jet index

a. Index definition

To facilitate analysis of GPLLJ variability, an index is constructed from areal averaging of the meridional wind in a 5° × 10° longitude–latitude box (25°–35°N, 102°–97°W). The box is chosen to encompass the core sectors of the meridional wind and moisture flux climatologies, including many local maxima.[4] The wind vertical level in index definition is chosen after inspection of the vertical profile of the box-averaged meridional wind.

Figure 5 shows the April–August NARR profiles and the July ERA-40 profile, all of which exhibit the classic low-level jet structure. The coarser vertical resolution (75 hPa) ERA-40 data places the wind maximum at 850 hPa and is a bit challenged in depicting vertical shear, especially in comparison with the 25-hPa-resolution NARR data. The NARR southerly flow is strongest at 900 hPa in all months, which helps with the choice of level in index definition. The southerly jet is especially strong in May, June, and July, and thus only these months (MJJ) will be considered in the following interannual variability analysis. The GPLLJ index is finally defined as the box-averaged 900-hPa meridional wind.

b. Index variations

Figure 6 plots the GPLLJ index *anomalies* from ERA-40 and NARR datasets. The top two panels show the ERA-40 index anomalies; the display period is broken into two panels to facilitate comparison with the

[3] It is interesting that the northward moisture flux associated with the Gulf of California low-level jet is maximum full 1–2 months after the GPLLJ-related flux attains its peak.

[4] The sensitivity to longitudinal averaging was assessed by computing correlations of indices generated using slightly shifted boxes; correlations are ~0.95. Note the coarser-resolution Bonner (1968) GPLLJ climatology indicates 95°–100°W as the sector of maximum meridional winds, that is, very close to the longitude range identified here.

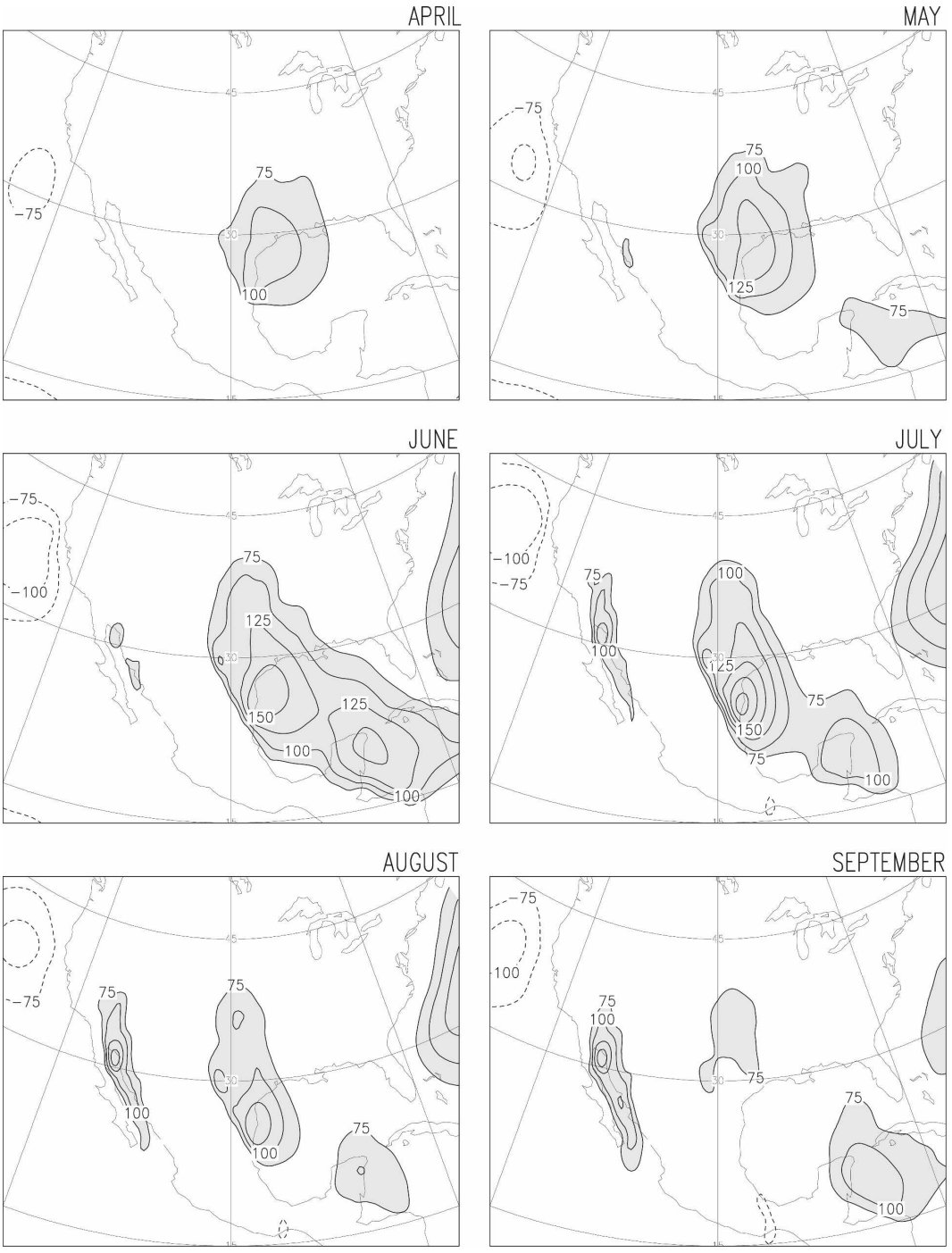

FIG. 3. Seasonal evolution of the 1000–700-hPa integrated meridional water vapor flux in NARR. Contour interval is 25 kg m^{-1} s^{-1} and values in excess of 75 kg m^{-1} s^{-1} are shaded. Horizontal resolution is the same as in Fig. 1.

NARR index anomalies (bottom panel) in the overlapping data period (1979–2001).[5] The GPLLJ index has substantial intraseasonal variability, switching sign in 28 of the 40 ERA-40 summers. During the common period, the ERA-40 index exhibits 16 sign changes as opposed to 14 in NARR. Monthly indices in NARR and ERA-40 are strong and reasonably consistent. The monthly standard deviation is 0.98 in ERA-40 and 1.20

[5] The ERA-40 index was computed using the 925-hPa winds, that is, winds at the closest archive level to 900 hPa.

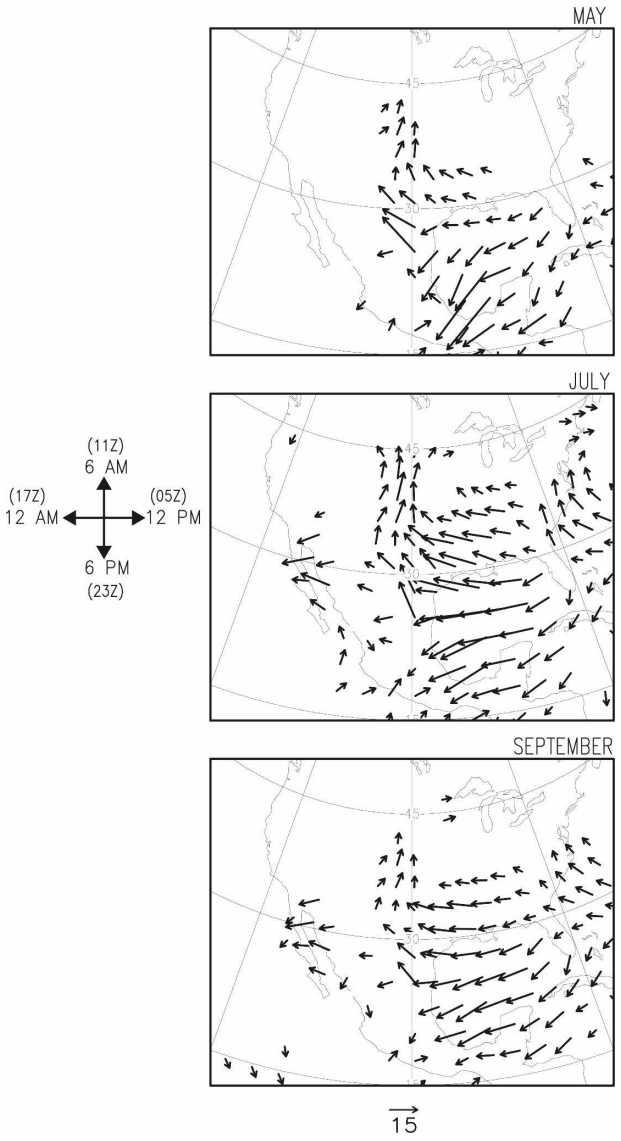

FIG. 4. Seasonal evolution of the diurnal amplitude and phase of the 1000–700-hPa integrated meridional water vapor flux in NARR. Units are m^{-1} s^{-1}. Direction of the arrow determines local time of maximum amplitude. Arrow length denotes magnitude. Horizontal resolution is the same as Fig. 1.

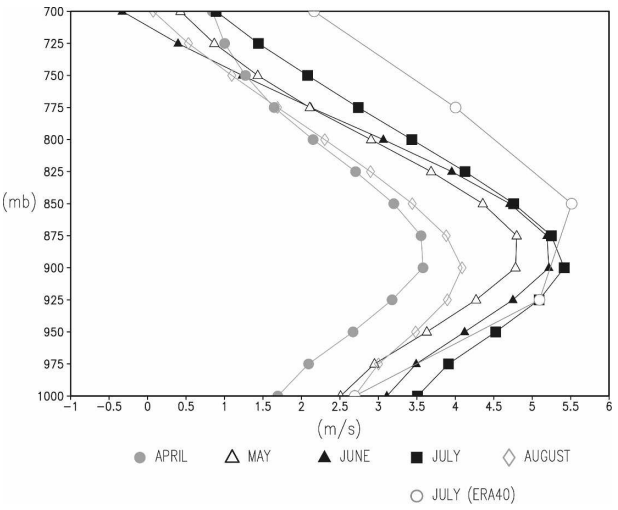

FIG. 5. Vertical profile of the GPLLJ as reflected in the area-averaged (25°–35°N, 102°–97°W) meridional wind for the warm season months of April–August in NARR. For July, ERA-40 is included for comparison. The vertical resolution is 25 hPa in NARR and 75 hPa in ERA-40. Units are m s^{-1}.

in NARR, and the common period correlation is a robust 0.97, indicating remarkably similar representation of GPLLJ variability in modern global and regional reanalyses. The May–July (July only) GPLLJ and Great Plains precipitation indices are correlated at 0.55 (0.71).

An interesting feature of the GPLLJ index is its characterization of the 1988 drought and 1993 floods. The index is most negative in the overlapping period in June 1988; note that a negative index denotes a weakened GPLLJ and reduced northward moisture flux. On the other hand, the index is large and positive in 1993 June and July; indicating a stronger jet and related moisture transports.[6]

Interannual variability of the index is highlighted by the superposed bold lines in Fig. 6, which were generated by a 1–2–1 smoothing of the seasonal (MJJ) index anomalies. Focusing on lower frequencies, the GPLLJ exhibited a maximum in early 1960s followed by a weakening trend until the 1980s. The jet was weakest in 1988 and has been gradually strengthening since then.

5. GPLLJ's circulation and hydroclimate links

Indices are a widely used simple statistic for characterizing regional variability and links with other variables and regions. The GPLLJ index is used in developing a comprehensive view of regional climate variability related to jet variations, through computation of index regressions during the MJJ months, a period in which jet variability is fairly uniformly distributed: standard deviation of the May, June, and July GPLLJ index is 1.32, 1.09, and 1.08 m s^{-1}. Precipitation variability is also uniformly distributed in these months: the Great Plains precipitation index standard deviations are 1.1, 1.09, and 1.08 mm day^{-1}, respectively.

Although the circulation and precipitation standard

[6] It is interesting to note that the extremely high index value in 1996 was not coincident with an anomalously wet summer (cf. Fig. 3a in RBN05).

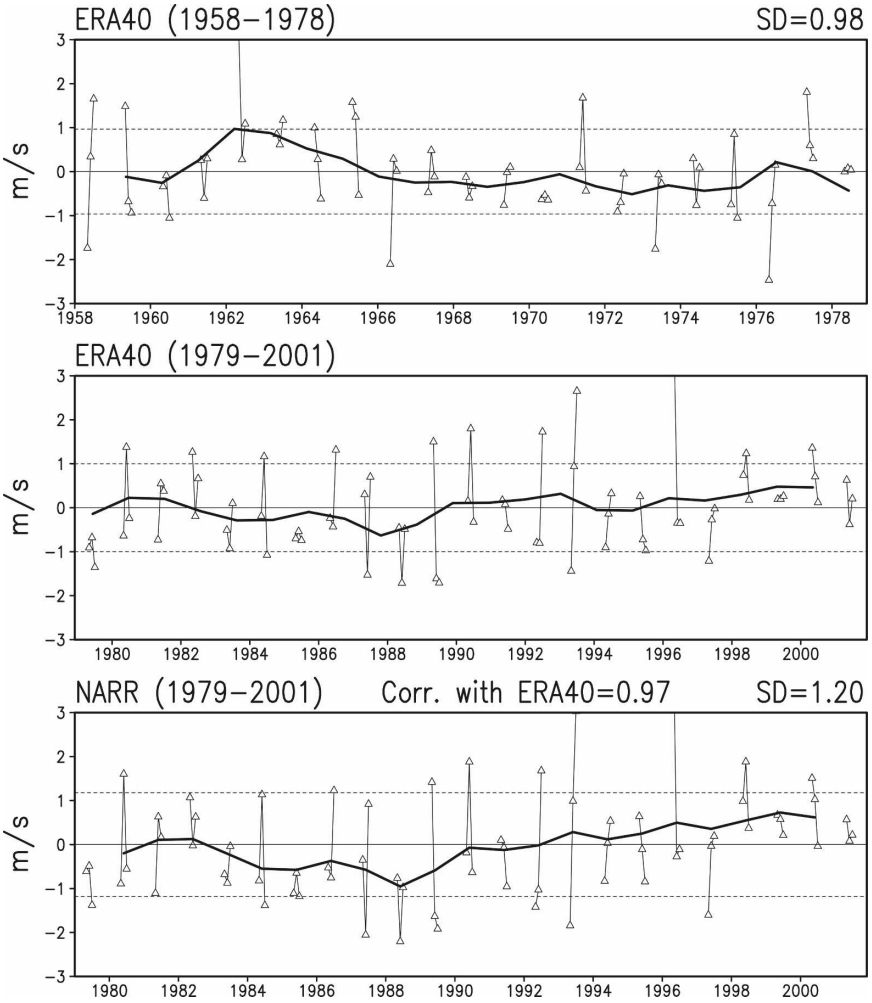

FIG. 6. GPLLJ index anomalies during the warm season (May–July) in (top) ERA-40 (1958–1978, (middle) ERA-40 (1979–2001), and (bottom) NARR (1979–2001). Monthly values are shown using a triangle, while the smoothed index obtained from a 1–2–1 averaging of the seasonal mean anomalies is displayed using solid lines. Horizontal dashed lines mark the ±1 std dev range in each panel.

deviations are fairly uniformly distributed in MJJ months, the circulation–precipitation links are generally manifest in June and July; for example, the notable GPLLJ anomalies in May of 1962 and 1996 (cf. Fig. 6) are not associated with significant hydroclimate episodes. In contrast, jet anomalies in June 1988 and July 1993 are both linked with notable precipitation anomalies. With July exhibiting maximum GPLLJ amplitude and significant interannual variability, and given that July has historically represented summer conditions, an expansive view of LLJ variability is developed from the July index regressions. The July regressions however need not be characteristic of other summer months for various reasons, including the dependence of climate teleconnections on the seasonally evolving background flow.

a. Precipitation

Index regressions on the 900-hPa NARR meridional winds are shown in Fig. 7a. Southerly anomalies are present over the central United States, with maximum values along the northeastern edge of the index box, indicating a slight eastward (westward) shift of the strengthened (weakened) GPLLJ. Jet intensification is also accompanied by northerly anomalies off the west and east coasts of Canada, indicating that jet modulation occurs in the context of continental-scale circulation anomalies. The index regressions on NARR and ERA-40 precipitation are shown in Figs. 7b and 7d, respectively. The precipitation regressions differ considerably in both structure and magnitude, not surprisingly, since NARR assimilates observed precipitation

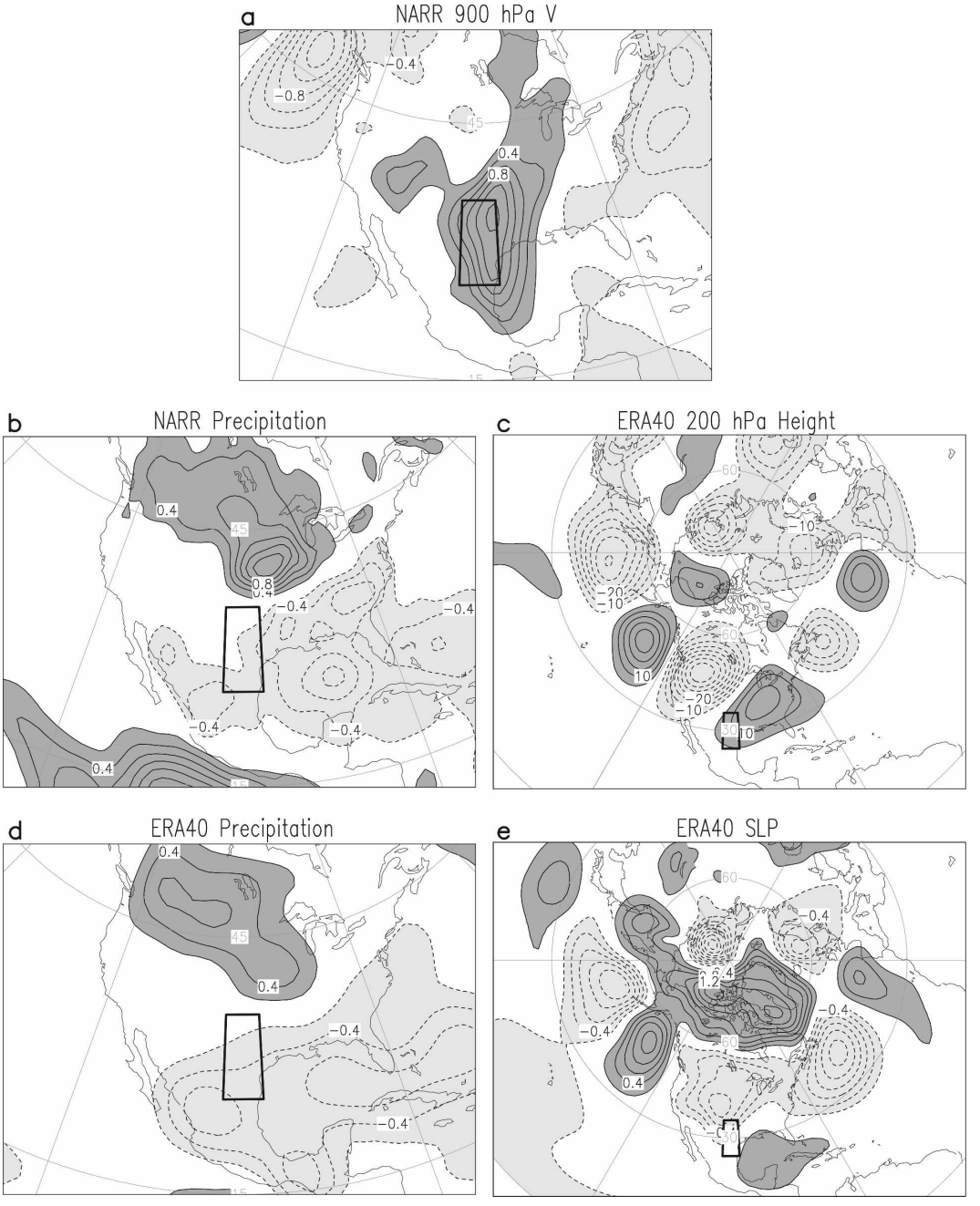

FIG. 7. July regressions of the GPLLJ index (1979–2001) on NARR (a) 900-hPa wind and (b) precipitation, and ERA-40 (c) 200-hPa geopotential height, (d) precipitation, and (e) sea level pressure. Contour interval for wind is 0.2 m s^{-1}, height is 5 m. Precipitation and SLP contours are 0.2 mm day^{-1} and 0.2 hPa, respectively. In all panels dark (light) shading denotes positive (negative) values. The rectangular box outlines the area defined by the GPLLJ index.

while ERA-40 generates its own from a forecast. The jet strengthening is associated, not surprisingly, with positive precipitation anomalies (~1.5 mm day^{-1}) in the jet-exit region, where climatological precipitation is ~3 mm day^{-1}; the precipitation anomaly is thus quite significant. The downstream location of the precipitation anomaly is consistent with previous studies showing low-level convergence and ascending motions in the jet-exit region. Oppositely signed but smaller anomalies are present over the southeastern states and the Gulf of Mexico.

b. Circulation

The GPLLJ index regressions on 200-hPa geopotential height and SLP are shown in Figs. 7c,e; the regressions are on ERA-40 data.[7] The height regressions show a coherent wave pattern over the North Pacific–North American region and over the midlatitude Atlantic. The pattern suggests that the GPLLJ can be influenced by the hemispheric-scale summertime teleconnection patterns, assuming robust lower-tropospheric extensions of these upper-level anomalies, the case given the structure of sea level pressure regressions. Regressions obtained from the June index (not shown) contain similar patterns except for the sign of the height and SLP anomalies in the western Pacific and Atlantic basins. Aspects of the remote influence are thus somewhat sensitive to the choice of the month, but not the three-cell height pattern of consequence for the GPLLJ, the one with centers over eastern North Pacific, western North America, and southeastern United States, which is present in all summer month regressions.

It is noteworthy that this height pattern bears strong resemblance to the summertime stationary wave pattern forced by western Pacific diabatic heating (along with secondary interaction with North American orography) in a linear baroclinic model and a GCM (Ting 1994). Specifically noted was an orographically forced wave train (an alternating high–low–high pattern) emanating from the Rockies, with downstream extensions over the southeastern United States and the North Atlantic. An enhancement of this very feature is seen in Fig. 7c regressions. The observed 200-hPa height anomalies in the North Pacific–North American region during the notably wet Midwest summer of 1993 (cf. Fig. 3 in Liu et al. 1998) are almost identical to those shown in Fig. 7c, except for the amplitude differences.

The sea level pressure associated with GPLLJ variability (Fig. 7e) shows a coherent pattern in the North Pacific–North American region similar to the overlying 200-hPa height pattern (Fig. 7c). This equivalent barotropic structure of the anomalies—a characteristic feature of the far-field (i.e., far from the wave source) stationary wave response (e.g., Held 1983)—in the North Pacific–North American region argues for the significance of remote forcing of GPLLJ variability. The GPLLJ-related anomalies in the Atlantic also exhibit equivalent barotropic structure, not withstanding the weak 200-hPa high over northeastern Canada.[8]

c. NAO

Sea level pressure anomalies in the Atlantic also exhibit coherent structure, but one reminiscent of the North Atlantic Oscillation (NAO) in winter. Given that the NAO is a robust mode of winter variability, most studies have focused on characterizing NAO structure and impacts during this season, including index development to mark winter NAO variability. The variability is however not confined to the winter season: sea level pressure variability with meridional-dipole structure in the extratropical Atlantic basin, closely mimicking the NAO winter structure, is manifest in other seasons too, including summer, as here. NAO variability in summer was also recently noted in context of Great Plains hydroclimate variability (RBN05).

Monitoring NAO variability in seasons other than winter is however not straightforward. The canonical NAO index (e.g., Hurrell 1995) cannot be indiscriminately used as it is based on the structure of winter sea level pressure variability. Although a summer NAO index can be developed employing the strategy used for the winter index, a 700-hPa geopotential-based NAO index is used for comparative analysis here. The index was developed at the National Oceanic and Atmospheric Administration's (NOAA's) Climate Prediction Center from EOF analysis of height variability in summer (http://www.cpc.ncep.noaa.gov/data/teledoc), and as such, appropriate for use here; in addition to being readily available.

The link between GPLLJ and NAO variability, suggested by SLP regressions in Fig. 7e, is reexamined, this time from the NAO perspective. The NAO's influence on GPLLJ and regional hydroclimate is directly assessed in Fig. 8, from regressions of the July NAO index. The sea level pressure footprint is shown first (top panel) and is evidently very similar to the GPLLJ index regressions in the Atlantic (Fig. 7e); pattern correlation in the American–Atlantic sector (20°–70°N, 110°W–0°) is −0.8, supporting the claim of linkage between GPLLJ and NAO variability. The linkage is probed further via NAO index regressions on NARR meridional wind and precipitation fields. The regressions exhibit cohesive structure that is strikingly similar to that found in GPLLJ index regressions (Figs. 7a,b), except for the sign. It is interesting that while the NAO influ-

[7] The ERA-40 fields are used here in order to identify the hemispheric-scale linkages, something not feasible with regional NARR data.

[8] The positive height anomalies are not fleshed out in this region, perhaps because the 200-hPa level is above the tropopause here.

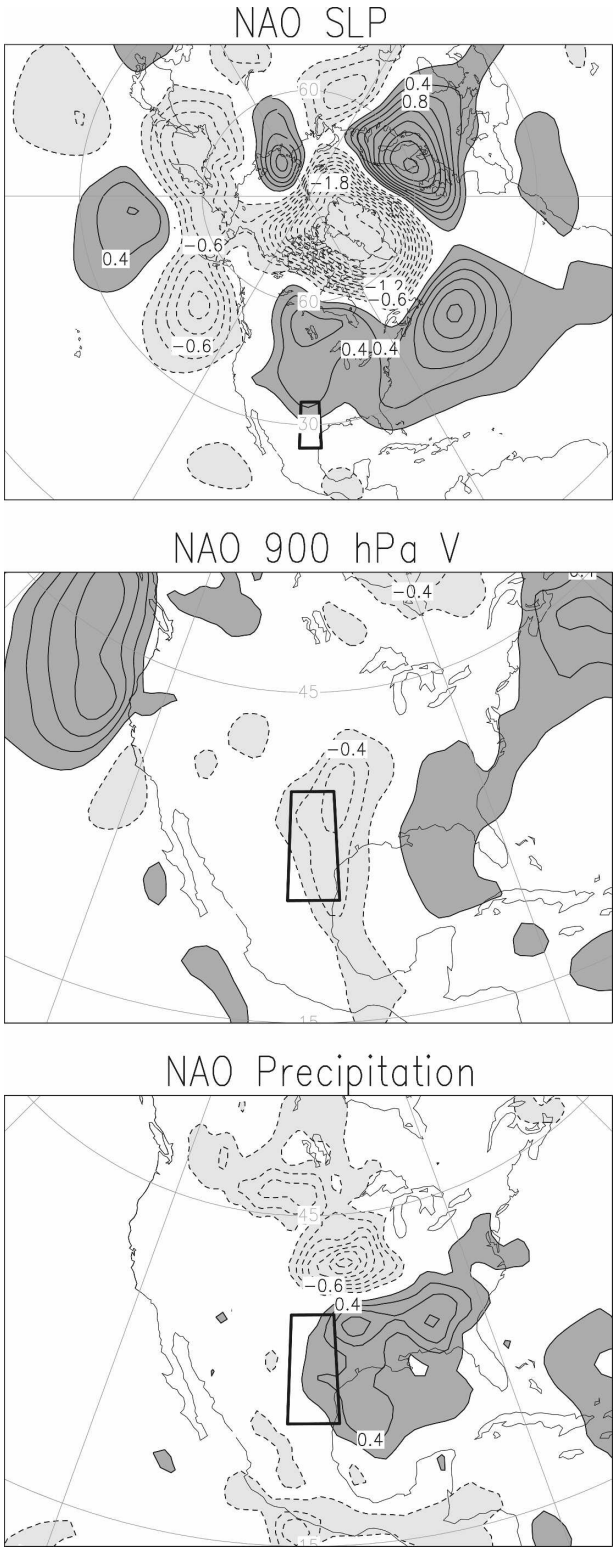

ence on the GPLLJ is modest (~0.5 m s^{-1}, i.e., about half the amplitude of that in Fig. 7a), its influence on Great Plains rainfall (~1.2 mm day^{-1}) is substantial and comparable to that in Fig. 7b.

Despite considerable correspondence between the GPLLJ and NAO index regressions, the two July indices are temporally correlated at −0.46, that is, rather modestly. The reason for this is not entirely clear but the possibility that the GPLLJ index reflects a superposition of variability modes (as it must), not all of which are hydroclimate sensitive, is currently being investigated. Notwithstanding this concern, this section's analysis buttresses our claim of significant links between NAO summer variability and Great Plains hydroclimate. Dynamically, the link is fostered by modulations of the most prominent feature of the Atlantic's summertime sea level pressure distribution, the Bermuda high (see RBN05).

d. Diabatic heating

Although coherent wave patterns in the Pacific and Atlantic sectors in Figs. 7 and 8 make the case for remote forcing of GPLLJ variability, the nature/location of forcing that generate these wave patterns (and GPLLJ variability) remains to be elucidated. The forcing is examined in Fig. 9 from GPLLJ index regressions on July's diabatic heating. Vertically averaged diabatic heating is shaded in Fig. 9a while the Rossby wave source is contoured. Significant heating anomalies are present in the western-central (and eastern) tropical Pacific as well as over Central America and the Gulf of Mexico. The heating anomalies, including diminished heating over Nordeste, resemble heating distribution in the post El Niño summer. Characteristic ENSO heating distributions are, unfortunately, available mostly for winter (Nigam et al. 2000). Characteristic ENSO precipitation, from which tropical diabatic heating anomalies can be inferred, is however available for all four seasons in a Web supplement of Joseph and Nigam (2006; http://www.atmos.umd.edu/~nigam/renu/main_frame.htm). Inspection of the December–February (DJF) Niño-3 regressions on the following

←

FIG. 8. July regressions of the NAO index on (top) SLP in ERA-40, (middle) 900-hPa meridional winds, and (bottom) precipitation in NARR. In all panels dark (light) shading denotes positive (negative) values. The contour interval in the top panel is 0.2 hPa, while in the middle and lower panels it is 0.2 m s^{-1} and 0.2 mm day^{-1}, respectively. The rectangular box outlines the area defined by the GPLLJ index.

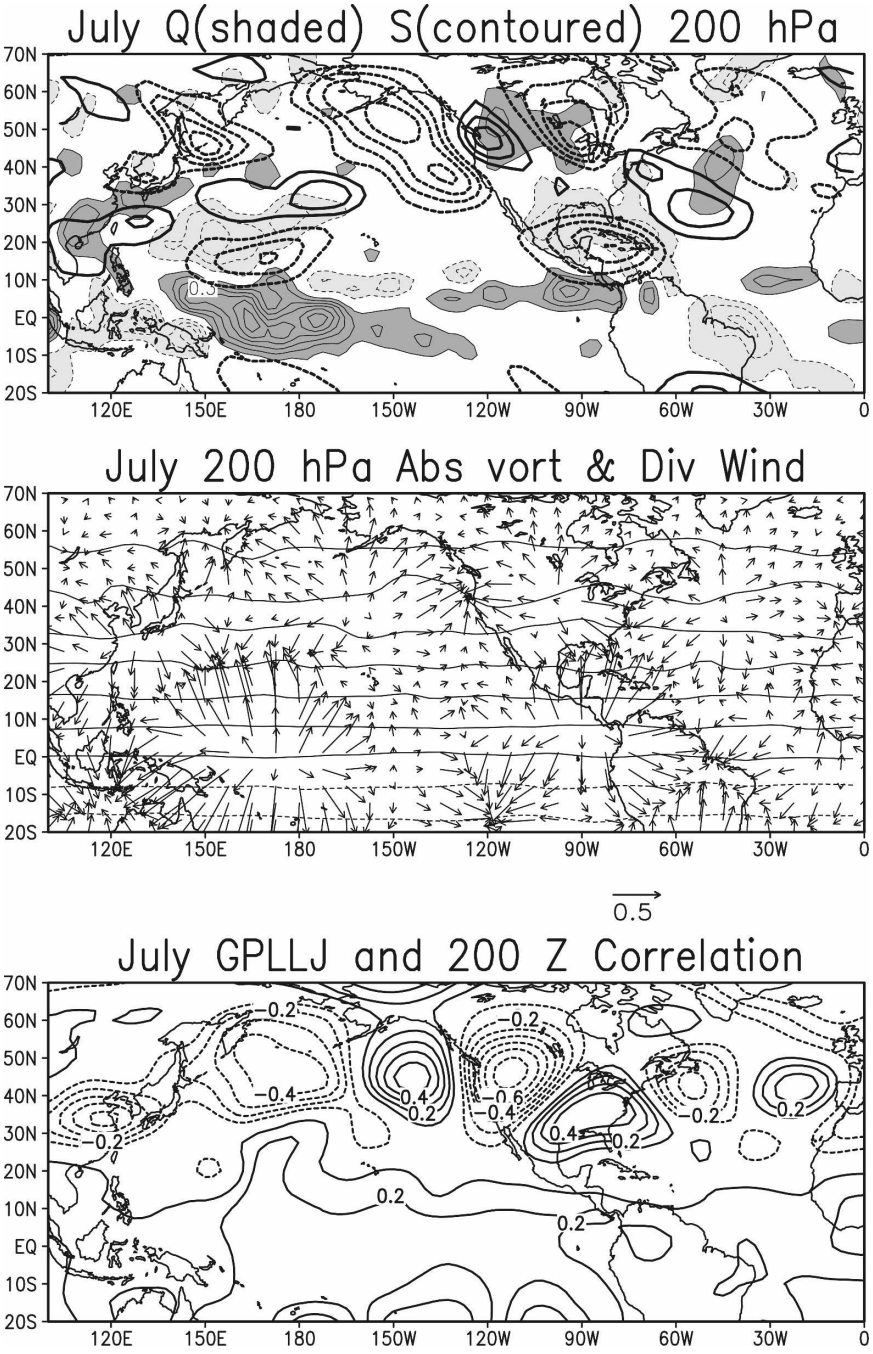

FIG. 9. July regressions of the GPLLJ index on (top) 1000–200-hPa average diabatic heating and the Rossby wave source, (middle) 200-hPa divergent winds and absolute vorticity, and (bottom) July correlations of the GPLLJ index on 200-hPa height. Diabatic heating contours are 0.1 K day^{-1}, and dark (light) shading denotes positive (negative) values. The Rossby wave source is contoured for positive (solid) and negative (dashed) values. Divergent winds are displayed using arrows (reference vector is 0.5 m s^{-1}). Absolute vorticity is contoured at 10^{-5} s^{-1}.

June–August (JJA) precipitation reveals some similarity with the Fig. 9a heating distribution.

Although tropical heating is the progenitor of significant climate anomalies across the globe, the underlying circulation teleconnections are dynamically instigated not directly from regions of deep tropical outflow but from adjacent subtropical ones determined by the Rossby wave source (RWS; Sardeshmukh and Hoskins

1988). The Rossby wave source, as the name implies, is the source or forcing term for Rossby waves in the barotropic vorticity equation.

The RWS contains terms involving divergent flow: $\text{RWS} = -\nabla \cdot (\mathbf{v}'_\chi \zeta_c) - \nabla \cdot (\mathbf{v}_{\chi c} \zeta')$, where $\mathbf{v}_\chi$ is the divergent component of the wind, ζ is the absolute vorticity ($\eta + f$), and primes and subscript "c" denote anomaly and climatology, respectively. The first term on the rhs is generally dominant and can be expressed as the sum of a tropical ($-\mathbf{v}'_\chi \cdot \nabla \zeta_c$) and extratropical ($-\zeta_c \nabla \cdot \mathbf{v}'_\chi$) RWS component (e.g., Qin and Robinson 1993). Given the meridional reach of tropical divergent outflows ($\mathbf{v}'_\chi$), the RWS can be large thousands of kilometers northward of an equatorial diabatic heating anomaly, especially in the western Pacific sector, where meridional vorticity gradients ($\nabla \zeta_c$) are large in the extratropics due to the presence of the Asian–Pacific jet.

The 200-hPa absolute vorticity and divergent winds are shown in Fig. 9b. The equatorial divergent outflow centers in the western and eastern Pacific basin, coincident with positive diabatic heating anomalies, stand out. The wave sources arising from these outflows are prominent features in the northern subtropics of the top panel: the negative RWS in the western-central Pacific and Central American longitudes. Note the RWS distribution in the middle and high latitudes is part of the quasigeostrophic response itself, and as such, not insightful about the wave emanation (or source) regions.

What does the RWS analysis tell us about remote forcing of the GPLLJ height regressions? Inspection of the RWS distribution suggests that both of the negative sources noted above are influential in instigating the July height regression pattern (Fig. 7c). While the height regression structure itself is not suggestive of these links, this is not surprising since geopotential is not a variable of choice in tropical–extratropical teleconnections analysis given that height gradients are very weak in the tropics on account of the smallness of the Coriolis parameter there. As such, streamfunction is often used in lieu of the geopotential, or one can simply compute height correlations (and not regressions). The height correlations (Fig. 9c) are much more strongly suggestive of tropical links, especially in the longitudinal sectors of the above noted RWS sources.

The Great Plains low-level jet thus appears susceptible to remote influences, including those originating in the western-central subtropical Pacific, in addition to the more local ones originating to the south. Although specific attribution is beyond the scope of this diagnostic study, Ting's (1994) analysis of the influence of Pacific SST anomalies, and Ding and Wang's (2005) and Lau and Weng's (2002) recent analyses linking Great Plains precipitation with teleconnection patterns emanating from tropical Pacific and Asian regions, are insightful in this regard.

e. *Subseasonal versus interannual regression contributions*

The GPLLJ index exhibits both subseasonal and interannual variability. The sign change of the index in most summers suggests that subseasonal variability will make a significant contribution to index regressions. This subseasonal contribution was ascertained from regressions of a modified GPLLJ index; the modification involved subtracting the seasonal (May–July) anomaly from each month of that season. Regressions of the modified index are very similar to those displayed in Fig. 7, and thus not shown. The similarity reflects the dominance of subseasonal influence in index regressions, especially in regional fields; for example, the subseasonal contribution to GPLLJ and Great Plains precipitation variability (Figs. 7a,b) is ~80%. The contribution to upper-level height and sea level pressure regressions in the Pacific longitudes is not as overwhelming though. While the subseasonal, interannual apportioning of the response is helpful, it does not, necessarily, convey the relative importance of forcing at these time scales; for example, ENSO SSTs can elicit a subseasonal response from monthly evolution of the background flow (e.g., Opsteegh and Van den Dool 1980).

6. Recurrent patterns of GPLLJ variability

An index is a widely used simple statistic to track regional variability. While its simplicity is attractive, it is not without some costs, especially when the region of interest is the locus of several variability patterns. In such situations, the index represents a superposition of variability patterns, and as such, index regressions cannot be counted upon to provide insights into the operative mechanisms. Given our interest in the latter, an EOF analysis is conducted to identify the recurrent patterns of GPLLJ variability.

a. *EOF analysis: Three modes of variability*

The EOF analysis was conducted on monthly 900-hPa NARR meridional wind anomalies in the 20°–50°N and 105°–85°W domain, for the May, June, and July months. The domain was chosen to fully encompass the jet core and its precipitation impacts. The left column of Fig. 10 displays the first three EOFs (contoured) atop

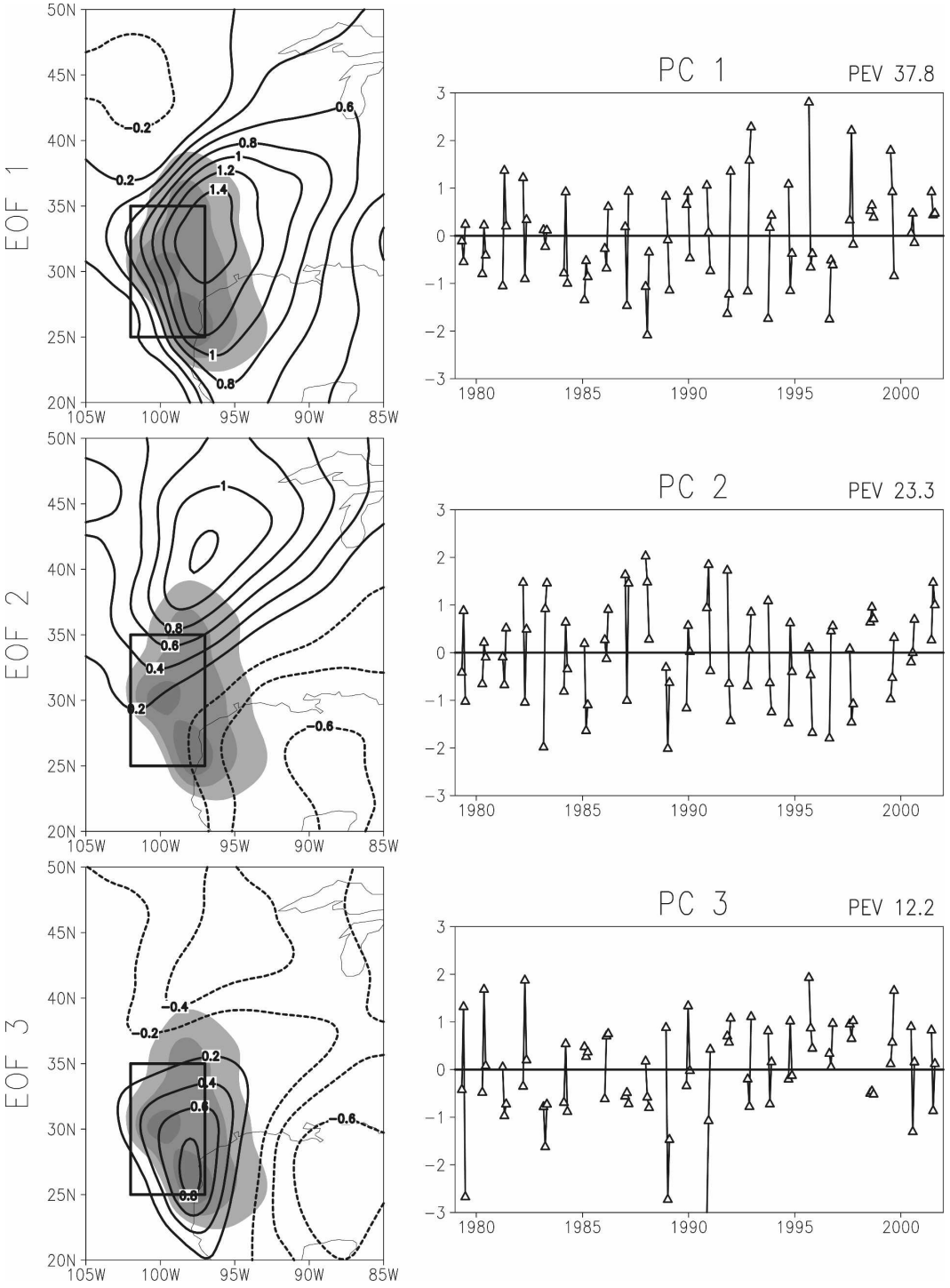

FIG. 10. Recurring patterns of MJJ GPLLJ variability. (left) MJJ 900-hPa wind climatology (shaded) and the first three EOF modes (contours) for MJJ. Meridional wind climatology values in excess of 4 m s^{-1} are shaded at 1 m s^{-1} intervals. The contour interval for the EOF spatial patterns is 0.2 m s^{-1}. (right) MJJ principal component time series associated with each mode is displayed with percentages of explained variance.

the climatological MJJ 900-hPa meridional wind (i.e., the climatological GPLLJ, which is shaded when >5 m s^{-1}); the corresponding principal components (PCs) are in the right column. The three leading EOFs explain 37.8%, 23.3%, and 12.2% of the regional meridional wind variance, respectively.

The leading mode of variability (mode 1) is characterized by substantial strengthening and spatial expansion of the jet core. Although there is a northward shift of the core, the meridional expansion of the jet keeps it tied to the moisture source, the Gulf of Mexico. The enhanced core-region jet speed should result in stronger low-level convergence in the jet-exit region and thus precipitation (as shown later in Fig. 12a). An inspection of PC1 shows substantial intraseasonal variability, with the PC switching sign in 19 of the 24 analyzed summers. PC1 is most negative in June 1988 and strongly positive in June–July 1993, coincident with severe drought and floods over central United States in those summers. This PC should be well correlated with the GPLLJ index on account of significant v_{900} amplitude in the GPLLJ index box, and it is, at 0.86.

Mode 2 represents a significantly northward-shifted GPLLJ, much more than in mode 1. The negative values over northern Gulf of Mexico, along with anomaly-core location at 40°–45°N, effectively isolate the perturbed GPLLJ from the Gulf moisture source. The PC2 distribution shows this mode to be in positive phase during the 1988 summer. There is more intraseasonal variability manifest in PC2 as evidenced by sign changes in 21 of the 24 analyzed summers. Given the weak meridional wind amplitudes in the marked index box, PC2 is weakly correlated with the GPLLJ index (-0.15).

In contrast with modes 1 and 2, mode 3 shows an in-place strengthening of the climatological GPLLJ, along with reduced meridional flow over central–northern Great Plains, that is, a meridional dipole anomaly. In the positive phase, northward moisture flux is enhanced over the western Gulf from increased jet speed but diminished over the central-eastern sectors of the Gulf, which is under the influence of climatology-opposing meridional wind anomalies in this phase. Strengthening (weakening) of the climatological LLJ is associated with floods (droughts) in the central United States due to enhanced (suppressed) moisture flux convergence, as seen later from the modal precipitation links (Fig. 12). The PC3 distribution indicates that mode 3 was not notably anomalous during the 1988 and 1993 summers, indicating a modest role for this mode of GPLLJ variability in the recent prominent hydroclimate episodes.[9] PC3 is modestly correlated with the GPLLJ index (0.46).

b. *Stability of EOF analysis*

The stability of the identified GPLLJ variability patterns was assessed from EOF analysis of variability in the much longer (40+ yr) ERA-40 dataset (1958–2001). The coarser resolution of ERA-40 data vis-à-vis NARR data was a concern but not an overwhelming one given the opportunity to assess pattern stability. Figure 11 shows the second-leading EOF from the ERA-40-based analysis, which should be compared with the second-left panel in Fig. 10; this EOF was chosen for intercomparison because of its interesting height regressions. Intercomparison indicates remarkable structural robustness of this variability pattern, which is the case for the other patterns, as well. To be sure, there are amplitude differences—ERA-40's are weaker—but some are, undoubtedly, due to coarser ERA-40 data.

Also shown in Fig. 11 are the July height regressions of PC2: NARR PC2 regressions on ERA-40 heights (1979–2001) are in the upper panel, while the ERA-40 PC2 regressions on ERA-40 heights (1958–2001) are in the bottom panel. The structural similarity of the large-scale patterns is notable, given the differences in regression period and, potentially, in the PCs themselves. The similarity attests to the robustness of regressions, not just in the analyzed variable (v_{900}), but also in related circulation and hydroclimate. The upper-level anticyclone over the north central United States is noteworthy given its prominence in U.S. droughts (Bell and Janowiak 1995; Mo et al. 1997).

It is interesting to compare the PC2 height regressions with the GPLLJ index ones (Fig. 7c). The index regressions depict a zonally oriented, coherent wave pattern with limited connectivity to the tropics–subtropics, while the PC ones have an arching structure with greater connectivity; one that is, to an extent, manifest even in the height field. The U.S. features in the two regressions are also in spatial quadrature. These differences suggest that while the GPLLJ index can be a useful fulcrum for many analyses, it is not suitable for probing mechanisms generating GPLLJ variability.

c. *PC regressions on precipitation*

Figure 12 shows NARR PC regressions on NARR's July precipitation. The PC1 regressions in northern

[9] All three PCs are positive in July 1993.

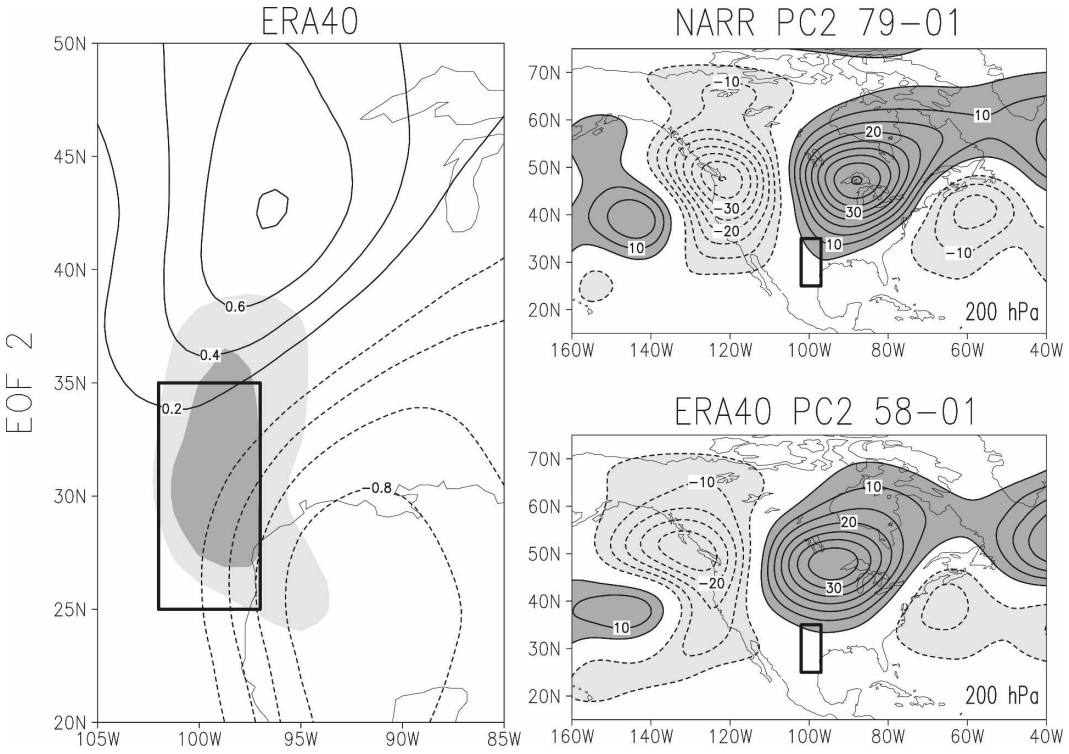

FIG. 11. Sensitivity of GPLLJ EOF modes to time period. (left) EOF 2 (contoured) from principal component analysis and MJJ climatology (shaded; same as in Fig. 11) of ERA-40 900-hPa meridional winds. (right) PC2 regression on July 200-hPa height in both (top) NARR and (bottom) ERA-40. The EOF contour interval is 0.2 m s^{-1}, and the 200-hPa height regressions are contoured at 5 m. The NARR regression is over the 1979–2001 time period, while the ERA-40 one is over 1958–2001. The rectangular box outlines the area defined by the GPLLJ index.

plains are large (~1.5 mm day^{-1}) and their structure very similar to the GPLLJ index regressions (Fig. 7b), not surprising, given the 0.86 correlation between PC1 and the index. The precipitation pattern linked with PC2 (middle panel) is more focused over the Gulf coast states and eastern seaboard, where anomalies are ~0.8 mm day^{-1}, and Mexico. Unlike PC1, PC2 regressions have a meridional dipole structure between the GPLLJ entrance and exit regions. PC2's correlation with the GPLLJ index is modest (−0.15) as noted before, but the mode is important for Gulf states' precipitation variability. The bottom panel displays the PC3 regressions, which show diminished precipitation over south-central United States, Mexico, and the Gulf of Mexico, along with modest positive amplitudes over the Great Plains. It is interesting that despite similar meridional wind structure along Mexico's Gulf coast in modes 1 and 3, their local precipitation footprints are so different. Clearly, meridional wind divergence ($\partial v/\partial y$) alone cannot account for mode 3's negative precipitation anomalies. Of the three modes, only 2 and 3 evidently influence Mexican rainfall.

7. Discussion and concluding remarks

This study has sought to characterize the variability of the low-level circulation feature that transports vast amounts of moisture and heat from the Gulf of Mexico into the continental interior during the late spring and summer months: the Great Plains low-level jet. Much has been written about the GPLLJ, especially its remarkable diurnal variability, which includes a nocturnal maximum. The low-level jet is however more than a supplier of moisture to the Great Plains: the jet's strength, shear, and related divergent circulations influence the timing, location, and intensity of precipitation in the continental interior (Stensrud 1996).

Unlike most studies of the jet, which focus on its mesoscale structure and dynamics, the present study characterizes GPLLJ variability, regional precipitation impacts, and its larger-scale circulation links using monthly averaged data. Jet studies with monthly data would have been considered heretical up until a few decades ago, when spatially and temporally sparse observations would either be unable to represent many

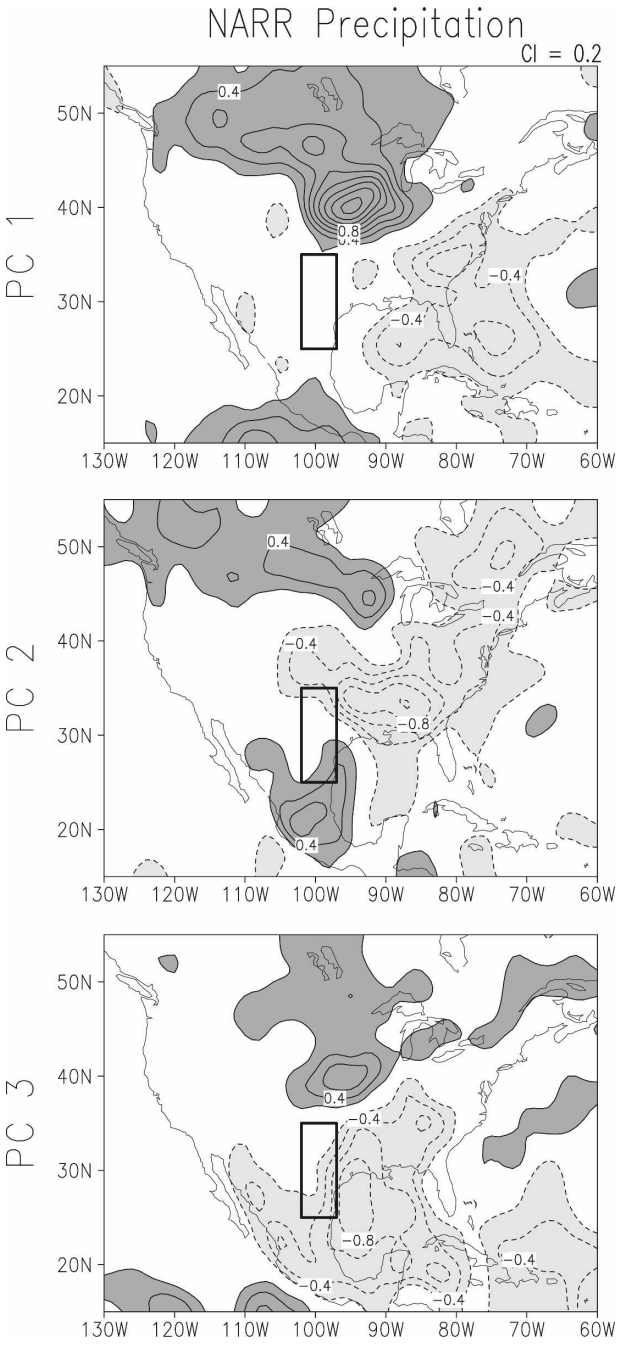

FIG. 12. GPLLJ principal component regressions on NARR precipitation during July. The contour interval is 0.2 mm day^{-1}. Dark (light) shading indicates positive (negative) values. The rectangular box outlines the area defined by the GPLLJ index.

features of this vertically shallow and meridionally narrow jet; or if they did, the jet structure stood a reasonable chance of getting diluted, or even wiped out, upon monthly averaging of sparse observations, limiting any subsequent analysis.

Monthly analysis of GPLLJ structure, variability, and regional hydroclimate impacts became feasible with the recent availability of a high-resolution (32-km horizontal resolution, 25-hPa PBL resolution, 3-hourly) precipitation-assimilating regional reanalyses over North America (NARR). The goal of this study is to uncover the monthly variability structure of the GPLLJ in NARR (and ERA-40) data and investigate the large-scale circulation context and origin of GPLLJ variability. The principal findings are as follows:

- Diurnal range of the jet in 3-hourly monthly NARR climatology shows latitude dependence, with the nighttime-to-daytime speed ratio increasing with latitude.
- GPLLJ variability is reasonably captured by the average 900-hPa meridional wind anomalies in the climatological jet-core region (25°–35°N, 102°–97°W), defining the GPLLJ index.
- GPLLJ index shows both subseasonal and interannual variability. NARR and ERA-40 indices are correlated at 0.97 in the overlapping record. Index fluctuations mark recent droughts and floods. The GPLLJ index and Great Plains precipitation index are correlated 0.71 in July.
- Index regressions on July sea level pressure and 200-hPa geopotential show coherent large-scale patterns over the North Pacific–North American region and the midlatitude Atlantic basin, indicating GPLLJ's susceptibility to remote influences.
- Index regressions on diabatic heating suggest a role for the tropics in generation of GPLLJ variability. A Rossby wave source analysis indicates the western-central and eastern tropical Pacific sectors to be potential wave source regions.
- EOF analysis of GPLLJ variability shows the jet index to be composed of three modes that, together, account for ~75% of the variance. The modes represent the following:
  - strengthening/expansion of the jet core (38%), with strong precipitation impact on the northern Great Plains;
  - meridional shift of the GPLLJ (23%), with a Gulf states precipitation focus;
  - in-place strengthening of the GPLLJ (12%), with dipolar influence on Great Plains and Gulf states precipitation, and linked to summer NAO variability.

Advancing the hydroclimate prediction accuracy over United States, especially for the agriculturally sensitive warm season, will remain challenging unless one reckons with the variability and predictability of the

Great Plains low-level jet, the conduit for massive moisture transports from the Gulf of Mexico into the heartland. Remote influences from the Pacific and Atlantic basins (and other regions) can influence continental hydroclimate, generally, in one of two ways: by directly influencing the moisture transport or the thermodynamic environment, which governs the extraction of moisture.

The present study has characterized the former influence through analysis of the structure and origin of GPLLJ variability, including quantitative estimation of the Pacific and Atlantic basin influences. Dynamical and thermodynamical mechanisms generating the remote influences and ensuing jet modulations is the subject of ongoing analysis, predicated on lead/lag linkages of pentad-averaged circulation and hydroclimate data.

Acknowledgments. We thank Alfredo Ruiz-Barradas, Chi-Fan Shih (NCAR), and the NCAR Scientific Computing Division. Sumat Nigam wishes to acknowledge support of Grants NOAA/CPPA NA17EC1483 and NSF ATM-0649666.

REFERENCES

Barlow, M., S. Nigam, and E. H. Berbery, 1998: Evolution of the North American monsoon system. *J. Climate,* **11,** 2238–2257.

Bell, G. D., and J. E. Janowiak, 1995: Atmospheric circulation associated with the Midwest floods of 1993. *Bull. Amer. Meteor. Soc.,* **76,** 681–695.

Blackadar, A. K., 1957: Boundary layer wind maxima and their significance for the growth of nocturnal inversions. *Bull. Amer. Meteor. Soc.,* **38,** 283–290.

Bonner, W. D., 1968: Climatology of the low level jet. *Mon. Wea. Rev.,* **96,** 833–850.

Byerle, L. A., and J. Paegle, 2003: Modulation of the Great Plains low-level jet and moisture transports by orography and large-scale circulations. *J. Geophys. Res.,* **108,** 8611, doi:10.1029/2002JD003005.

Ding, Q., and B. Wang, 2005: Circumglobal teleconnection in the Northern Hemisphere summer. *J. Climate,* **18,** 3483–3505.

Held, I. M., and D. G. Andrews, 1983: On the direction of the eddy momentum flux in baroclinic instability. *J. Atmos. Sci.,* **40,** 2220–2231.

Helfand, H. M., and S. D. Schubert, 1995: Climatology of the simulated Great Plains low-level jet and its contribution to the continental moisture budget of the United States. *J. Climate,* **8,** 784–806.

Higgins, R. W., Y. Yao, E. S. Yarosh, J. E. Janowiak, and K. C. Mo, 1997: Influence of the Great Plains low-level jet on summertime precipitation and moisture transport over the central United States. *J. Climate,* **10,** 481–507.

Holton, J. R., 1967: The diurnal boundary layer wind oscillation above sloping terrain. *Tellus,* **19,** 199–205.

Hornberger, G. M., and Coauthors, 2001: A plan for a new science initiative of the global water cycle. U.S. Global Change Research Program, 118 pp. [Available online at http://www.usgcrp.gov/usgcrp/Library/watercycle/wcsgreport2001/default.htm.]

Hoskins, B. J., H. H. Hsu, I. N. James, M. Masutani, P. D. Sardeshmukh, and G. H. White, 1989: Diagnostics of the global atmospheric circulation based on ECMWF analyses 1979–1989. WCRP-27, WMO Tech. Doc. 326, 217 pp.

Hoxit, L. R., 1975: Diurnal variations in planetary boundary-layer winds over land. *Bound.-Layer Meteor.,* **8,** 21–38.

Hurrell, J. W., 1995: Decadal trends in the North Atlantic Oscillation: Regional temperatures and precipitation. *Science,* **269,** 676–679.

Joseph, R., and S. Nigam, 2006: ENSO evolution and teleconnections in IFCC's twentieth-century climate simulations: Realistic representation? *J. Climate,* **19,** 4360–4377.

Lau, K.-M., and H. Weng, 2002: Recurrent teleconnection patterns linking summertime precipitation variability over East Asia and North America. *J. Meteor. Soc. Japan,* **80,** 1309–1324.

Liu, A. Z., M. Ting, and H. Wang, 1998: Maintenance of circulation anomalies during the 1988 drought and 1993 floods over the United States. *J. Atmos. Sci.,* **55,** 2810–2832.

Mesinger, F., and Coauthors, 2006: North American Regional Reanalysis. *Bull. Amer. Meteor. Soc.,* **87,** 343–360.

Mo, K. C., J. Nogues-Paegle, and J. Paegle, 1995: Physical mechanisms of the 1993 summer floods. *J. Atmos. Sci.,* **52,** 879–895.

——, ——, and W. Higgins, 1997: Atmospheric processes associated with summer floods and droughts in the central United States. *J. Climate,* **10,** 3028–3046.

Nigam, S., 1994: On the dynamical basis for the Asian summer monsoon rainfall–El Niño relationship. *J. Climate,* **7,** 1750–1771.

——, C. Chung, and E. DeWeaver, 2000: ENSO diabatic heating in ECMWF and NCEP–NCAR reanalyses, and NCAR CCM3 simulation. *J. Climate,* **13,** 3152–3171.

Opsteegh, J. D., and H. M. Van den Dool, 1980: Seasonal differences in the stationary response of a linearized primitive equation model: Prospects for long-range weather forecasting? *J. Atmos. Sci.,* **37,** 2169–2185.

Pan, Z., M. Segal, and R. W. Arritt, 2004: Role of topography in forcing low-level jets in the central United States during the 1993 flood-altered terrain simulations. *Mon. Wea. Rev.,* **132,** 396–403.

Qin, J., and W. A. Robinson, 1993: On the Rossby wave source and the steady linear response to tropical forcing. *J. Atmos. Sci.,* **50,** 1819–1823.

Rayner, N. A., P. Brohan, D. E. Parker, C. K. Folland, J. J. Kennedy, M. Vanicek, T. J. Ansell, and S. F. B. Tett, 2006: Improved analyses of changes and uncertainties in sea surface temperature measured in situ since the mid-nineteenth century: The HadSST2 dataset. *J. Climate,* **19,** 446–469.

Ruiz-Barradas, A., and S. Nigam, 2005: Warm season rainfall variability over the U.S. Great Plains in observations, NCEP and ERA-40 reanalyses, and NCAR and NASA atmospheric model simulations. *J. Climate,* **18,** 1808–1830.

Sardeshmukh, P. D., and B. J. Hoskins, 1988: The generation of global rotational flow by steady idealized tropical divergence. *J. Atmos. Sci.,* **45,** 1228–1251.

Schubert, S. D., H. M. Helfand, C.-Y. Wu, and W. Min, 1998: Subseasonal variations in warm-season moisture transport and precipitation over the central and eastern United States. *J. Climate,* **11,** 2530–2555.

Stensrud, D. J., 1996: Importance of low-level jets to climate: A review. *J. Climate,* **9,** 1698–1711.

Ting, M., 1994: Maintainance of northern summer stationary waves in a GCM. *J. Atmos. Sci.,* **51,** 3286–3308.

——, and H. Wang, 2006: The role of the North American topography on the maintenance of the Great Plains summer low-level jet. *J. Atmos. Sci.,* **63,** 1056–1068.

Trenberth, K. E., and C. J. Guillemot, 1996: Physical processes involved in the 1988 drought and 1993 floods in North America. *J. Climate,* **9,** 1288–1298.

Uccellini, L. W., and D. R. Johnson, 1979: The coupling of upper and lower tropospheric jet streaks and implications for the development of severe convective storms. *Mon. Wea. Rev.,* **107,** 682–703.

Uppala, S. M., and Coauthors, 2005: The ERA-40 re-analysis. *Quart. J. Roy. Meteor. Soc.,* **131,** 2961–3012.

Wexler, H., 1961: A boundary layer interpretation of the low level jet. *Tellus,* **13,** 368–378.

Zhang, D.-L., S. Zhang, and S. J. Weaver, 2006: Low-level jets over the Mid-Atlantic states: Warm season climatology and a case study. *J. Appl. Meteor.,* **45,** 194–209.

Zhong, S., J. D. Fast, and X. Bian, 1996: A case study of the Great Plains low-level jet using wind profiler network data and a high-resolution mesoscale model. *Mon. Wea. Rev.,* **124,** 785–806.